



Published in final edited form as:

Nat Chem Biol. 2011 May ; 7(5): 278–284. doi:10.1038/nchembio.545.

Retromer terminates the generation of cAMP by internalized PTH-receptors

Timothy N. Feinstein¹, Vanessa L. Wehbi¹, Juan Ardura¹, David S. Wheeler¹, Sebastien Ferrandon², Thomas J. Gardella², and Jean-Pierre Vilardaga^{1,2,†}

¹ Laboratory for GPCR Biology, Department of Pharmacology and Chemical Biology, University of Pittsburgh, School of Medicine, Pittsburgh, PA 15261, USA

² Endocrine Unit, Department of Medicine, Massachusetts General Hospital and Harvard Medical School, Boston, MA 02114, USA

Abstract

Generation of cAMP by G protein-coupled receptors (GPCRs) and its termination is currently thought to occur exclusively at the plasma membrane of cells. Under existing models of receptor regulation, this signal is primarily restricted by desensitization of the receptors through their binding to β -arrestins. However, this paradigm is not consistent with recent observations that the parathyroid hormone receptor type 1 (PTHr) continues to stimulate cAMP production even after receptor internalization, as β -arrestins are known to rapidly bind and internalize activated PTHr. Here we show that β -arrestin1 binding prolongs rather than terminates cAMP generation by PTHr, and that cAMP generation correlates with the persistence of arrestin-receptor complexes on endosomes. We found that PTHr signaling is instead turned-off by the retromer complex, which regulates traffic of internalized receptor from endosomes to the Golgi apparatus. Thus, binding by the retromer complex regulates sustained cAMP generation triggered by an internalized GPCR.

The production of cAMP by activated GPCRs is traditionally thought to originate exclusively at the plasma membrane. In most receptors studied to date elevated cAMP is rapidly extinguished by mechanisms that desensitized activated receptors through phosphorylation by G protein receptor kinases, arrestin binding that prevents further G protein coupling and can recruit cAMP specific phosphodiesterases (PDE4D) to the plasma membrane¹, and receptor endocytosis², after which desensitized receptors are recycled to the

Users may view, print, copy, download and text and data-mine the content in such documents, for the purposes of academic research, subject always to the full Conditions of use: http://www.nature.com/authors/editorial_policies/license.html#terms

[†]Corresponding author: Jean-Pierre Vilardaga, Ph. D., Department of Pharmacology and Chemical Biology, E1357 Thomas E. Starzl Biochemical Science Tower, 200 Lothrop Street, Pittsburgh, PA 15261, Tel: (412) 648 2055, Fax: (412) 648 1945, jpv@pitt.edu.

Note: Supplementary information is available on the Nature Chemical Biology website.

Competing interests statement

The authors have no competing financial interests to disclose.

Author contributions

T.N.F. performed most of the experiments with the support of V.L.W., J.A., D.S.W., S.F., and T.J.G.; J.-P.V. designed and supervised the experiments; J.-P.V. and T.N.F. analyzed the data and wrote the manuscript; all authors discussed the results and commented on the manuscript.

plasma membrane or trafficked to lysosomes for degradation³. In either case, production of cAMP is not thought to continue after GPCR internalization. However, recent studies have shown that cAMP production mediated by the PTHR in response to PTH or PTH analogs continues even after internalization of the activated receptor^{4,5}. Together with recent work on the thyroid-stimulating hormone receptor^{6,7}, these observations indicate that a number of GPCRs continue to signal after agonist-induced internalization using a presently unknown mechanism that does not conform to existing models. These studies therefore challenge the commonly held assumption that cAMP production by GPCRs occurs and terminates solely at the cytoplasmic side of the plasma membrane.

PTHr is a critical receptor for bone development and mineral ion homeostasis, and is a target for current and proposed drugs to treat bone and mineral disorders such as osteoporosis^{8–10}. PTHR regulates these cell functions primarily by activating two types of G-protein, G_s and G_q, which in turn activate adenylyl cyclases/cAMP/PKA and phospholipase C/inositol phosphates (IP3)/PKC signaling cascades, respectively. Like many GPCRs, PTHR binds β-arrestins and internalizes rapidly after activation^{11–14}. Recent evidence, however, indicates that certain PTH analogs such as M-PTH(1–28) induce prolonged physiological responses (calcemic and phosphate) *in vivo*⁵, a process thought to be associated with the capacity of PTHR to generate cAMP for many minutes after internalization of the receptor-ligand complex into early endosomes along with adenylyl cyclases and G_s^{4,15}. These data present strong evidence to question whether either arrestin-receptor binding or PTHR internalization are responsible for terminating PTH-induced cAMP production. It is also unlikely that PTHR is downregulated by degradation, as activated PTHR does not colocalize with late endosome markers⁴. Based on these observations, we hypothesize that an unrecognized mechanism turns off cAMP generation triggered by PTH. Here we show that retromer, a multimeric complex involved in retrograde protein transport from early endosomes to the Golgi, desensitizes cAMP generated by PTHR in response to PTH binding in both bone and kidney-derived cell lines.

RESULTS

Regulation of PTHR signaling by arrestin

Initial experiments assessed the effect of arrestin function on PTHR-mediated calcium ion (Ca²⁺) and cAMP responses in live cells. We first examined whether depletion of both β-arrestin1 and β-arrestin2 expression by siRNA (Supplementary Results, Supplementary Fig. 1) influences the capacity of PTH(1–34), a synthetic analog of naturally circulating PTH(1–84), to increase intracellular Ca²⁺ concentrations ([Ca²⁺]_i), and cAMP production (Fig. 1a,b). Depletion of β-arrestins in human embryonic kidney (HEK293) cells stably expressing PTHR resulted in longer intracellular Ca²⁺ transients after a brief exposure (< 10 s) to a saturating concentration (100 nM) of PTH(1–34) (Fig. 1a). We found that the integrated calcium response was significantly increased (*P* < 0.05) (Fig. 1c). We next measured the time course of PTH-mediated cAMP signaling using a FRET-based biosensor, epac^{CFP/YFP}, which has been previously described¹⁶. This cAMP biosensor displays a dynamic range of ~ 0.1–10 μM¹⁷ and its maximal response mediated by a saturating concentration of PTH (1 μM) is 92 ± 2.5% of that mediated by forskolin (10 μM). Cyclic

AMP generation persisted at elevated levels for ~20 minutes after ligand washout in control cells, consistent with previous reports^{4,5} (Fig. 1b). The cAMP response was much shorter in cells depleted of β -arrestins (Fig. 1c), and the integrated cAMP response for 30 minutes after ligand washout was significantly reduced ($P < 0.001$) (Fig. 1c). These results are consistent with arrestin-mediated decoupling of PTHR-G_q signaling. However, they do not support a model in which arrestin decouples PTHR signaling via G_s.

Earlier studies showed that overexpressed β -arrestins bind and mediate internalization of PTH(1–34)/PTH_R complexes without inhibiting cAMP levels, although β -arrestins overexpression did block the generation of inositol phosphates (IP₃)¹². In agreement with this, we found that overexpressed β -arrestin1 did not shorten the generation of cAMP in response to PTH(1–34). Rather, the cAMP level lasted longer in cells overexpressing β -arrestin1 than in controls (Fig. 2a). Overexpression of β -arrestin1 did inhibit cAMP generation by the β_2 -adrenergic receptor (β_2 -AR) in response to isoproterenol (Supplementary Fig. 2), in agreement with numerous reports^{18,21} showing that arrestin decouples signaling by the β_2 -AR. These data suggest that the regulation of PTHR signaling occurs by distinct mechanisms.

PTH_R/arrestin complexes and duration of cAMP signaling

The prolonged cAMP response caused by β -arrestin1 overexpression prompted us to analyze the dependence between the stability of the PTHR-arrestin complex and the duration of cAMP responses.

First, we investigated the action of N-terminal PTH analogs modified with a series of “M” substitutions (M=Ala/Aib¹, Aib³, Gln¹⁰, Har¹¹, Ala¹², Trp¹⁴, Arg¹⁹) that induce longer or shorter biological response *in vivo*⁵. For this, we used HEK293 cells stably expressing PTHR and compared cAMP responses and the subcellular localization of receptor-arrestin complexes mediated by either a short-acting signaling ligand (M-PTH(1–14)), or a long-acting signaling ligand (M-PTH(1–28)). Each ligand induced a rapid and comparable elevation of cAMP as measured by FRET (Fig. 2a,b). After ligand washout, the cAMP response induced by M-PTH(1–14) returned rapidly to the basal level, whereas cAMP induced by PTH(1–34) or M-PTH(1–28) remained elevated for many minutes after ligand washout (Fig. 2a,b). The cAMP signal induced by M-PTH(1–28) was longer than that induced by PTH(1–34) (Fig. 2a), in agreement with the capacity of M-PTH(1–28) to prolong physiological responses mediated by PTHR⁵. We observed that cAMP response induced by PTH(1–34) or M-PTH(1–28) remained sustained at times when nearly all of PTHR-arrestin complexes visualized by GFP^{PTH_R} (GFP inserted in the PTHR’s N-terminus) and β -arr1^{tom} (tdTomato fused to β -arr1), had internalized to endosomal domains (Fig. 2c and Supplementary Fig. 3). At comparable time points (20–40 min) PTHR-arrestin complexes induced by M-PTH(1–14) were not found in internalized compartments and arrestin was homogeneously distributed in the cytosol, indicating that arrestin dissociated rapidly from PTHR after washout of M-PTH(1–14). We verified the relative stability of PTHR-arrestin complexes induced by different ligands by measuring intermolecular FRET between PTHR^{CFP} and β -arrestin1^{YFP} transiently expressed in HEK293 cells. Application of either PTH(1–34), M-PTH(1–14) or M-PTH(1–28) caused a rapid increase in the FRET signal

(~10% elevation), which reflected the capacity of these PTHR ligands to stimulate PTHR-arrestin binding Supplementary Fig. 4b). After ligand washout, the FRET signal induced by M-PTH(1–14) rapidly diminished, whereas that induced by PTH(1–34) or M-PTH(1–28) was sustained. These data suggest that the longer elevation of cAMP observed in response to PTH(1–34) or M-PTH(1–28) is accompanied by persistent PTHR-arrestin complexes.

Second, we tested whether enhancing receptor-arrestin interactions would abbreviate or prolong the generation of cAMP. To do this, we used a mutant of β -arrestin1, I³⁸⁶A, V³⁸⁷A (hereafter noted, β -arr1[IV-AA], or β -arr1[IV-AA]^{tom} when tagged with tdTomato), that exhibits constitutive coupling to the adaptor protein AP2 subunit of clathrin^{22,23} and is stabilized in an active state that has increased binding affinity for ligand-activated GPCRs²³. Like β -arr1^{tom}, β -arr1[IV-AA]^{tom} rapidly colocalized with GFP^PPTHR at the plasma membrane in response to PTH(1–34) and cointernalized with the receptor to endosomes within 10–15 min (Fig. 2c and Supplementary Fig. 3). However, β -arr1[IV-AA]^{tom} remained colocalized with PTHR on endosomes for > 45 min after removal of the ligand. At this time point the cAMP signal mediated by PTH(1–34) was decreased by 40% in control cells and by 20% in cells overexpressing β -arr1^{tom}, but was undiminished in cells expressing β -arr1[IV-AA]^{tom} (Fig. 2a,b). These data indicated that increasing either the expression level of β -arrestin1 or its affinity for active PTHR enhances cAMP production.

Third, we tested whether prolonged generation of cAMP corresponds to an increase or a decrease in the stability of individual arrestin-receptor complexes. For this, we used dual color fluorescence recovery after photobleaching (FRAP) to measure whether the stability of arrestin-PTHR complexes on endosomes is linked to a longer cAMP production. After inducing formation and internalization of receptor-arrestin complexes in cells coexpressing GFP^PPTHR and β -arr1^{tom} with PTH(1–34), we bleached dTomato fluorescence on an endosome using a focused pulse of 561-nm laser light (Supplementary Fig. 5). Fluorescence recovery of dTomato was measured while fluorescence of GFP^PPTHR was used as a control to account for endosomal motion in X, Y and Z axes (Supplementary Fig. 5a). In separate experiments, tetramethylrhodamine-labeled PTH(1–34) (PTH^{TMR}) was used as a proxy for zero recovery, since the peptide ligand is topologically restricted to the lumen of endosomes. Wild type β -arr1^{tom} fluorescence recovered with a half-life ($t_{1/2}$) of 30 ± 2.5 s (Supplementary Fig. 5b). Thus, β -arrestin1 does not remain in a stable complex with PTHR, but instead cycles rapidly between endosomal membranes and the cytoplasm. Fluorescence recovery of endosomal β -arr1[IV-AA]^{tom} was not distinguishable from PTH^{TMR}, indicating that β -arr1[IV-AA] formed a tight complex with activated PTHR. Arrestin-PTHR complexes induced by M-PTH(1–28), the long acting analog of PTH(1–34), showed evidence of fluorescent recovery in the dTomato channel (Supplementary Fig. 5), however, the kinetic of fluorescence recovery ($t_{1/2} = 69 \pm 4.5$ s) was over three times slower ($P < 0.001$) than that recorded for arrestin after stimulation with PTH(1–34). Two lines of evidence therefore support a model in which stabilizing the arrestin-receptor complex prolongs rather than abbreviates cAMP signaling: a mutant of β -arrestin1 with increased receptor affinity, that also induces prolonged signaling, and a prolonged signaling-biased ligand that also induces more stable receptor arrestin-complexes.

Retromer modulates PTHR signaling

To understand how cAMP generation mediated by PTH is terminated, we examined the fate of PTHR during and after dissociation of PTHR-arrestin complexes on early endosomes. By time-lapse imaging we observed that ^{GFP}PTHR localized to a perinuclear organelle that we determined to be the Golgi apparatus by colocalization with the red fluorescent Golgi apparatus marker GRASP55^{mCherry} (Supplementary Fig. 6a) (ref.²⁴). Much of the ^{GFP}PTHR colocalized with GRASP55^{mCherry} within 30–40 min after a brief pulse of PTH(1–34) (Supplementary Fig. 6c). This observation is consistent with a recent report that internalized PTHR traffics to the Golgi apparatus in rat osteosarcoma cells²⁵.

We next tested whether trafficking of PTHR to the Golgi involves retromer, a heteropentameric complex consisting of two endosomal membrane-bound sorting nexins (Snx1 and Snx2) and a soluble heterotrimer (Vps26, Vps29, and Vps35) that regulates the sorting of a variety of transmembrane proteins from early endosomes to the Golgi^{26–28}. Overexpression of retromer subunits Vps26 and Vps35 significantly increased colocalization of ^{GFP}PTHR with the Golgi apparatus both before and after challenge with PTH(1–34) (Supplementary Fig. 4c). Conversely, depletion of the retromer subunit Vps35 using siRNA led to a marked reduction in receptor traffic to the Golgi (Supplementary Fig. 6b,c), supporting a role for retromer in sorting internalized PTHR to the Golgi.

We used a confocal microscope equipped for spectral deconvolution imaging^{29, 30} to simultaneously localize retromer, PTHR and arrestin in live cells after PTH(1–34) stimulation. For this, we coexpressed ^{GFP}PTHR, β -arr1^{tom} and the retromer subunit Vsp29^{YFP} in HEK293 cells and imaged individual endosomes at high resolution (40 nm/pixel) for 40 minutes after a 30 s challenge with PTH(1–34). Before ligand addition ^{GFP}PTHR was predominantly localized at the plasma membrane, and little to no colocalization was observed between PTHR and retromer or arrestin. A few minutes (< 15 min) after ligand stimulation, most endosomes ($83.4 \pm 2.5\%$, mean \pm s.e.m. of $N = 5$ experiments with $n = 50$ cells) labeled with internalized PTHR also contained both arrestin and retromer (Fig. 3a). These endosomes showed an extensive colocalization between arrestin and PTHR, but in these cases retromer did not co-localize with either PTHR or arrestin (Fig. 3a,b). At later time points (15–20 min) PTHR colocalized to a similar degree with both arrestin and retromer, whereas arrestin and retromer fluorescences remained largely distinct (Fig. 3a,b). This colocalization pattern can be clearly seen in a 3D reconstruction of an endosome taken at 20 min after ligand challenge (Supplementary Video 1). At still later time points (> 25 min) PTHR colocalized predominantly with retromer (Fig. 3b). Although arrestin and retromer typically labeled the same endosome (as determined by contiguous ^{GFP}PTHR fluorescence), we observed little to no colocalization between arrestin and retromer during the 60 min period after stimulation with PTH(1–34). This lack of overlap may be linked to a difference in phospholipid binding. It is known that retromer preferentially binds PI(3)P-enriched membrane domains³¹, whereas arrestin binding is enhanced in the presence of more negatively charged phospholipids such as phosphatidylinositol 3,5-bisphosphates (PI(3,4)P₂) (ref.³²). The transition of PTHR from arrestin- to retromer-labeled domains around 25 min after PTH(1–34) stimulation was confirmed using Pearson's analysis (Fig. 3b). On the other hand, when coexpressed with

β arr1[IV-AA]^{tom}, GFP^{PTH} remained localized in arrestin-specific endosomal domains for as long as 40 min after challenge with PTH(1–34) (Fig. 3b). These changes in PTHR localization are consistent with a gradual transfer of receptor from an arrestin-labeled compartment of the endosome to a retromer-labeled compartment dedicated to sorting cargo proteins into endosome-to-Golgi retrograde transport vesicles³¹.

Formation of a PTHR-retromer complex was also supported by co-immunoprecipitation experiments. For this, HA-tagged PTHR (PTH^{HA}) and Vps29^{YFP} were co-expressed in HEK293, and cell lysates were prepared at different time points after PTH(1–34) exposure. A low baseline interaction was detected when PTHR and retromer were coexpressed, possibly reflecting constitutive trafficking of a small fraction of PTHR^{33,34}. This interaction increased significantly by 15–25 min after challenge with PTH (Fig. 3c and Supplementary Fig. 7), consistent with our observations using colocalization (Fig. 3a,b).

As PTHR-retromer colocalization became prominent at roughly the same time (~25 min) that cAMP desensitization was observed, we tested the hypothesis that retromer may be involved in this desensitization process. The time course of cAMP generation stimulated by PTH(1–34) in HEK293 cells stably expressing PTHR and coexpressing the FRET-based cAMP sensor epac^{CFP/YFP}, along with retromer subunits myc-Vps26 and Vps29^{YFP}, was much shorter in cells overexpressing retromer than in controls. Depletion of retromer by siRNA resulted in prolonged cAMP signaling comparable with overexpression of β -arr1[IV-AA] (Fig. 4a). This inverse correlation between retromer protein levels and cAMP generation by PTHR is consistent with a model in which the generation of cAMP is terminated by interaction of PTHR with retromer on endosomes. When retromer was coexpressed with β -arr1[IV-AA], PTH(1–34)-induced cAMP generation was intermediate between signaling patterns induced by expressing either protein alone (Fig. 4b). Retromer overexpression did not reduce the number or affinity of plasma membrane-localized PTH receptors in cells overexpressing retromer (Supplementary Fig. 8), and had no effect on isoproterenol-mediated cAMP in HEK293 cells expressing β_2 -AR (Fig. 4c), a GPCR that generates a transient cAMP response due to rapid desensitization at the plasma membrane^{1,19}. These data rule out a non-specific role of retromer on cAMP signaling. It is therefore most likely that regulation of PTHR signaling occurs through a direct interaction between the receptor and retromer on endosomes.

We confirmed this conclusion in osteoblast-like ROS17/2.8 cells that natively express PTHR. Expression of β -arr1[IV-AA]^{tom} in ROS17/2.8 cells significantly prolonged a PTH-stimulated cAMP response relative to control cells (Fig. 5a), whereas the cAMP response was shortened by overexpression of retromer subunits Vps26 and Vps29 (Fig. 5a). In accordance with the effect of β -arrestin on the time course of cAMP in HEK-293 cells expressing the recombinant PTHR, we observed that PTH-induced cAMP production correlates strongly with expression of β arr1^{tom}, as measured using dTomato fluorescence (Fig. 5b).

Seminal studies showed that β -arrestins recruit cAMP-specific phosphodiesterase 4 (PDE4D) on activated β_2 -AR in the plasma membrane to rapidly degrade cAMP^{1,35}. However, activated ERK2 can also phosphorylate and inhibit PDE4³⁶. It is thus possible that

the sustained cAMP response observed with the PTHR-arrestin signaling system is due to the latter phenomenon, in which prolonged cAMP in PTH-stimulated cells is at least partly due to PDE4 inhibition by unusually stable receptor-arrestin complexes that prolong ERK1/2 activation. We found that the PTH(1–34)-dependent cAMP increase was prolonged by rolipram, a specific inhibitor of PDE4, and reduced by U0126, an inhibitor of MEK activation (Fig. 5c, and Supplementary Fig. 9). Additionally in ROS cells we found that PTH(1–34) induced a short decrease in ERK1/2 phosphorylation lasting less than 2 min, which is followed by a moderate increase. However, this initial decrease was followed by a significant elevation in ERK1/2 phosphorylation in cells transfected with β arr1[IV-AA] of ~3-fold over control levels (Fig. 5d and Supplementary Fig. 10). Based on these data we infer that the sustained generation of cAMP involves ERK1/2 activation.

Discussion

Our data shows that in both kidney and bone-derived cell lines, PTHR-arrestin complexes internalize to endosomes while still signaling via cAMP. Given that arrestin and G protein binding to receptors such as rhodopsin and the β_2 -AR are mutually exclusive^{20,21,37,38}, the present data raise the unavoidable question of how a stable PTHR-arrestin complex can continue to produce cAMP and thus couple to G_S . Our previous study shows that the interaction between $G\beta_1\gamma_2$ subunits and the PTHR, which is known to occur on the proximal domain of the long (132 amino acids) PTHR's carboxy-terminal tail^{39,40}, is maintained even when the PTH-bound receptor is internalized⁴. Additionally, the present data shows that β -arrestin1 forms a dynamic interaction with the PTH-PTHR complex, which nonetheless persists in endosomes for many cycles of receptor-arrestin association/dissociation. These results suggest that complexes formed through interactions between β -arrestin1 and $G\beta_1\gamma_2$ subunits, which are necessary for scaffolding signaling complexes⁴¹, might regulate the sustained cAMP signaling mediated by PTH by permitting multiple rounds of $G\alpha_S$ subunit coupling and activation, or stabilizing sustained coupling with the active state of $G\alpha_S$. Addressing these processes will require additional studies involving for example, the characterization of the assembly/disassembly dynamics of arrestin, and $G\beta\gamma$ with the receptor.

Although the mechanism of the sustained cAMP generation is not yet fully determined, our data present a new pathway for understanding how this sustained signaling is desensitized (Fig. 6). Our results shows that (1) retromer is associated with PTHR in early endosomes and shuttles it to the Golgi apparatus, (2) that retromer positively regulates the rate of retrograde endosome-to-Golgi PTHR traffic, (3) that retromer negatively regulates the duration of cAMP generation by PTHR, and finally, (4) that the relationship between retromer and β -arrestin is apparently competitive and entails a contest between signaling complexes of PTHR-arrestin and PTHR-retromer complexes that do not signal. In particular, the molecular basis for PTHR binding to retromer remains to be determined. This could be related to the structural similarity between the retromer subunit Vps26 and β -arrestins^{42,43}, and/or the scaffolding property of the Vps35 subunit, which serves as a scaffold for the currently known cargo⁴⁴ of retromer through an extended α -solenoid fold⁴⁵. Potentially supporting this alternative model, a short motif (FLN) located near the C-terminus of PTHR has some similarity to a motif in the cation-independent mannose-6-phosphate receptor

(WLM/FLV) that is necessary for binding Vps35⁴⁶. The new role of retromer, so far limited to intracellular sorting of cargo proteins such mannose-6-phosphate receptor⁴⁷, Wntless⁴⁸ and polymeric immunoglobulin receptors⁴⁹, has now expanded to include the regulation of the signaling and trafficking of a medically important GPCR. This model for PTHR regulation opens a new avenue to understand how the cell regulates GPCRs that generate cAMP from internal domains^{4,7}.

METHODS

Time-lapse confocal microscopy

Cells were grown on 25 mm polylysine-coated coverslips and transferred to an Attofluor chamber (Invitrogen, Carlsbad, CA) in HEPES/BSA buffer (HEPES buffer containing 0.1 % (w/v) BSA) for imaging at room temperature. Time-lapse movies were collected with a Nikon A1s confocal microscope attached to a Ti-E inverted base using a 60× 1.49 NA plan-apo objective. To minimize fluorescent bleed-through, all images were collected with a 32-PMT (Photo Multiplier Tubes) spectral detector and then processed using spectral deconvolution (Elements software, Nikon).

Fluorescence recovery after photobleaching (FRAP)

HEK293 cells expressing GFP^PPTHR were co-transfected with either wild-type β arrestin1^{tomato}, β arrestin1 (IV-AA)^{tomato} or challenged with red fluorescent PTH(1–34)^{TMR}. Initial fluorescence of endosomes was estimated from averaging three images taken immediately before bleaching. Red fluorescence was then immediately bleached using a 561 nm laser focused on a circular region of interest (1 mm diameter) encompassing the endosome. To avoid unnecessary photo-oxidation, laser power and bleach duration was calibrated before each experiment to bleach red endosomal fluorescence by 80–90%. Images were collected at 3–5 s. intervals for as long as the bleached endosome remained within the imaging plane (as determined by GFP fluorescence; typically ~ 1 min). Imaging in the GFP channel also accounted for endosome growth due to merger or vesicle traffic and served as a non-bleaching control. Intensity data for dTomato or TMR is presented after normalization to GFP intensity for each time point.

FRET

Cells plated on poly-D-lysine-coated glass coverslips and maintained in FRET buffer were placed on a Nikon Ti-E or a Zeiss (Axiovert 200) inverted microscope equipped with an oil immersion 60×NA 1.49 plan-apo objective and a dichroic beam splitter to allow simultaneous recording of CFP and YFP fluorescence channels (DualView2, Photometrics, Tucson, AZ, or TILL photonics, Germany). The emission fluorescence intensities were determined at 535 ± 15 nm (YFP) and 480 ± 20 nm (CFP) with a beam splitter DCLP of 505 nm. The FRET ratio for single experiments was corrected according to equation (1):

$$\text{Ratio} \left(\frac{F_{YFP}}{F_{CFP}} \right) = \frac{F_{YFP}^{ex436/em535} - a \times F_{CFP}^{ex436/em480} - b \times F_{YFP}^{ex500/em535}}{F_{CFP}^{ex436/em480}} \quad (1)$$

where $F_{YFP}^{ex436/em535}$ and $F_{CFP}^{ex436/em480}$ represent respectively the emission intensities of YFP (recorded at 535 nm) and CFP (recorded at 480 nm) upon excitation at 436 nm; a and b represent correction factors for the bleed-through of CFP into the 535 nm channel ($a = 0.35$) and the cross-talk due to the direct YFP excitation by light at 436 nm ($b = 0.06$). $F_{YFP}^{ex500/em535}$ represents the emission intensity of YFP (recorded at 535 nm) upon direct excitation at 500 nm, and was recorded at the beginning of each experiment. Note that bleed-through of YFP into the 480 nm channel was negligible. For each measurement, changes in fluorescence emissions due to photobleaching were subtracted. To ensure that CFP- and YFP-labeled molecule expression were similar in examined cells, we performed experiments in cells displaying comparable fluorescence levels.

The means of FRET experiments were calculated according to equation (2), which normalizes for different expression levels of CFP and YFP molecules:

$$N_{FRET} = \frac{F_{YFP}^{ex436/em535} - a \times F_{CFP}^{ex436/em480} - b \times F_{YFP}^{ex500/em535}}{\sqrt{F_{CFP}^{ex436/em480} \times F_{YFP}^{ex500/em535}}} \quad (2)$$

Note that in the epac-YFP/CFP the F_{YFP}/F_{CFP} ratio decreases upon generation of cAMP but its represented as a positive signal just for convenience.

Image deconvolution, quantitative image analysis and statistics

Spatial deconvolution of confocal images was performed using the Huygens Professional suite (Scientific Volume Imaging, Hilversum, the Netherlands). Images for deconvolution were taken according to manufacturer recommendations: Pixel size was 40×40 nm in X and Y dimensions, and 100 nm in the Z-axis when 3-dimensional image series were collected. Iterative deconvolution was then performed using a theoretical point spread function (PSF) based on entered values for objective NA, oil and medium refractive index, emission wavelength and estimated signal-to-noise ratio for each fluorophore.

Colocalization (Pearson's) was performed using integrated functions in Elements (Nikon) for raw confocal images. For spatially deconvolved endosomes, Pearson's colocalization coefficient was analyzed per endosome, per time point using the JACoP plugin for ImageJ after auto-thresholding.

Additional methods

Information on RNAi used and details of the cell culture, quantitative real-time PCR, intracellular calcium ion measurement, Western blots and immunoprecipitation, MAP kinase assay, and competition radioligand binding experiments can be founded in the Supplementary Methods.

Supplementary Material

Refer to Web version on PubMed Central for supplementary material.

Acknowledgments

This work was supported by the National Institutes of Health (NIH) award R01DK087688 (to J.-P.V.). We thank J. Bonifacino for the gift of plasmids encoding retromer subunits Vps26 and Vps29^{YFP}, and L. Traub for sharing the plasmids encoding β -arrestin1^{tom} and β -arrestin1[1386A, V387A]^{tom}.

References

1. Perry SJ, et al. Targeting of cyclic AMP degradation to beta 2-adrenergic receptors by beta-arrestins. *Science*. 2002; 298:834–6. [PubMed: 12399592]
2. Premont RT, Gainetdinov RR. Physiological roles of G protein-coupled receptor kinases and arrestins. *Annu Rev Physiol*. 2007; 69:511–34. [PubMed: 17305472]
3. Hanyaloglu AC, von Zastrow M. Regulation of GPCRs by endocytic membrane trafficking and its potential implications. *Annu Rev Pharmacol Toxicol*. 2008; 48:537–68. [PubMed: 18184106]
4. Ferrandon S, et al. Sustained cyclic AMP production by parathyroid hormone receptor endocytosis. *Nat Chem Biol*. 2009; 5:734–42. [PubMed: 19701185]
5. Okazaki M, et al. Prolonged signaling at the parathyroid hormone receptor by peptide ligands targeted to a specific receptor conformation. *Proc Natl Acad Sci U S A*. 2008; 105:16525–30. [PubMed: 18946036]
6. Robben JH, et al. Intracellular activation of vasopressin V2 receptor mutants in nephrogenic diabetes insipidus by nonpeptide agonists. *Proc Natl Acad Sci U S A*. 2009; 106:12195–200. [PubMed: 19587238]
7. Calebiro D, et al. Persistent cAMP-signals triggered by internalized G-protein-coupled receptors. *PLoS Biol*. 2009; 7:e1000172. [PubMed: 19688034]
8. Finkelstein JS, Arnold AL. Increases in bone mineral density after discontinuation of daily human parathyroid hormone and gonadotropin-releasing hormone analog administration in women with endometriosis. *J Clin Endocrinol Metab*. 1999; 84:1214–9. [PubMed: 10199756]
9. Neer RM, et al. Effect of parathyroid hormone (1–34) on fractures and bone mineral density in postmenopausal women with osteoporosis. *N Engl J Med*. 2001; 344:1434–41. [PubMed: 11346808]
10. Horwitz MJ, et al. Direct comparison of sustained infusion of human parathyroid hormone-related protein-(1–36) [hPTHrP-(1–36)] versus hPTH-(1–34) on serum calcium, plasma 1,25-dihydroxyvitamin D concentrations, and fractional calcium excretion in healthy human volunteers. *J Clin Endocrinol Metab*. 2003; 88:1603–9. [PubMed: 12679445]
11. Vilaradaga JP, et al. Internalization determinants of the parathyroid hormone receptor differentially regulate beta-arrestin/receptor association. *J Biol Chem*. 2002; 277:8121–9. [PubMed: 11726668]
12. Castro M, et al. Dual regulation of the parathyroid hormone (PTH)/PTH-related peptide receptor signaling by protein kinase C and beta-arrestins. *Endocrinology*. 2002; 143:3854–65. [PubMed: 12239097]
13. Ferrari SL, Behar V, Chorev M, Rosenblatt M, Bisello A. Endocytosis of ligand-human parathyroid hormone receptor 1 complexes is protein kinase C-dependent and involves beta-arrestin2. Real-time monitoring by fluorescence microscopy. *J Biol Chem*. 1999; 274:29968–75. [PubMed: 10514480]
14. Malecz N, Bambino T, Bencsik M, Nissenson RA. Identification of phosphorylation sites in the G protein-coupled receptor for parathyroid hormone. Receptor phosphorylation is not required for agonist-induced internalization. *Mol Endocrinol*. 1998; 12:1846–56. [PubMed: 9849959]
15. Rosenblatt M. When two keys fit one lock, surprises follow. *Nat Chem Biol*. 2009; 5:707–8. [PubMed: 19763099]
16. Nikolaev VO, Bunemann M, Hein L, Hannawacker A, Lohse MJ. Novel single chain cAMP sensors for receptor-induced signal propagation. *J Biol Chem*. 2004; 279:37215–8. [PubMed: 15231839]
17. Nikolaev VO, Hoffmann C, Bunemann M, Lohse MJ, Vilaradaga JP. Molecular basis of partial agonism at the neurotransmitter alpha2A-adrenergic receptor and Gi-protein heterotrimer. *J Biol Chem*. 2006; 281:24506–11. [PubMed: 16787921]

18. Pitcher J, Lohse MJ, Codina J, Caron MG, Lefkowitz RJ. Desensitization of the isolated beta 2-adrenergic receptor by beta-adrenergic receptor kinase, cAMP-dependent protein kinase, and protein kinase C occurs via distinct molecular mechanisms. *Biochemistry*. 1992; 31:3193–7. [PubMed: 1348186]
19. Violin JD, et al. beta2-adrenergic receptor signaling and desensitization elucidated by quantitative modeling of real time cAMP dynamics. *J Biol Chem*. 2008; 283:2949–61. [PubMed: 18045878]
20. Lohse MJ, Benovic JL, Codina J, Caron MG, Lefkowitz RJ. beta-Arrestin: a protein that regulates beta-adrenergic receptor function. *Science*. 1990; 248:1547–50. [PubMed: 2163110]
21. Lohse MJ, et al. Receptor-specific desensitization with purified proteins. Kinase dependence and receptor specificity of beta-arrestin and arrestin in the beta 2-adrenergic receptor and rhodopsin systems. *J Biol Chem*. 1992; 267:8558–64. [PubMed: 1349018]
22. Keyel PA, et al. The AP-2 adaptor beta2 appendage scaffolds alternate cargo endocytosis. *Mol Biol Cell*. 2008; 19:5309–26. [PubMed: 18843039]
23. Burtey A, et al. The conserved isoleucine-valine-phenylalanine motif couples activation state and endocytic functions of beta-arrestins. *Traffic*. 2007; 8:914–31. [PubMed: 17547696]
24. Feinstein TN, Linstedt AD. GRASP55 regulates Golgi ribbon formation. *Mol Biol Cell*. 2008; 19:2696–707. [PubMed: 18434598]
25. Garrido JL, Wheeler D, Vega LL, Friedman PA, Romero G. Role of phospholipase D in parathyroid hormone type 1 receptor signaling and trafficking. *Mol Endocrinol*. 2009; 23:2048–59. [PubMed: 19837945]
26. Collins BM, et al. Structure of Vps26B and mapping of its interaction with the retromer protein complex. *Traffic*. 2008; 9:366–79. [PubMed: 18088321]
27. Collins BM. The structure and function of the retromer protein complex. *Traffic*. 2008; 9:1811–22. [PubMed: 18541005]
28. Bonifacino JS, Rojas R. Retrograde transport from endosomes to the trans-Golgi network. *Nat Rev Mol Cell Biol*. 2006; 7:568–79. [PubMed: 16936697]
29. Zucker RM, Lerner JM. Wavelength and alignment tests for confocal spectral imaging systems. *Microsc Res Tech*. 2005; 68:307–19. [PubMed: 16315239]
30. Lerner JM, Zucker RM. Calibration and validation of confocal spectral imaging systems. *Cytometry A*. 2004; 62:8–34. [PubMed: 15468110]
31. Popoff V, et al. The retromer complex and clathrin define an early endosomal retrograde exit site. *J Cell Sci*. 2007; 120:2022–31. [PubMed: 17550971]
32. Gaidarov I, Krupnick JG, Falck JR, Benovic JL, Keen JH. Arrestin function in G protein-coupled receptor endocytosis requires phosphoinositide binding. *EMBO J*. 1999; 18:871–81. [PubMed: 10022830]
33. Chauvin S, Bencsik M, Bambino T, Nissenson RA. Parathyroid hormone receptor recycling: role of receptor dephosphorylation and beta-arrestin. *Mol Endocrinol*. 2002; 16:2720–32. [PubMed: 12456793]
34. Sneddon WB, et al. Activation-independent parathyroid hormone receptor internalization is regulated by NHERF1 (EBP50). *J Biol Chem*. 2003; 278:43787–96. [PubMed: 12920119]
35. Baillie GS, et al. beta-Arrestin-mediated PDE4 cAMP phosphodiesterase recruitment regulates beta-adrenoceptor switching from Gs to Gi. *Proc Natl Acad Sci U S A*. 2003; 100:940–5. [PubMed: 12552097]
36. Hoffmann R, Baillie GS, MacKenzie SJ, Yarwood SJ, Houslay MD. The MAP kinase ERK2 inhibits the cyclic AMP-specific phosphodiesterase HSPDE4D3 by phosphorylating it at Ser579. *EMBO J*. 1999; 18:893–903. [PubMed: 10022832]
37. Pippig S, et al. Overexpression of beta-arrestin and beta-adrenergic receptor kinase augment desensitization of beta 2-adrenergic receptors. *J Biol Chem*. 1993; 268:3201–8. [PubMed: 8381421]
38. Krupnick JG, Gurevich VV, Benovic JL. Mechanism of quenching of phototransduction. Binding competition between arrestin and transducin for phosphorhodopsin. *J Biol Chem*. 1997; 272:18125–31. [PubMed: 9218446]

39. Mahon MJ, Bonacci TM, Divieti P, Smrcka AV. A docking site for G protein $\beta\gamma$ subunits on the parathyroid hormone 1 receptor supports signaling through multiple pathways. *Mol Endocrinol.* 2006; 20:136–146. [PubMed: 16099817]
40. Johnston CA, Kimple AJ, Giguere PM, Siderovski DP. Structure of the parathyroid hormone receptor C terminus bound to the G-protein dimer G β 1 γ 2. *Structure.* 2008; 16:1086–94. [PubMed: 18611381]
41. Yang M, He RL, Benovic JL, Ye RD. beta-Arrestin1 interacts with the G-protein subunits beta1 γ 2 and promotes beta1 γ 2-dependent Akt signalling for NF-kappaB activation. *Biochem J.* 2009; 417:287–96. [PubMed: 18729826]
42. Shi H, Rojas R, Bonifacino JS, Hurley JH. The retromer subunit Vps26 has an arrestin fold and binds Vps35 through its C-terminal domain. *Nat Struct Mol Biol.* 2006; 13:540–8. [PubMed: 16732284]
43. Aubry L, Guetta D, Klein G. The arrestin fold: variations on a theme. *Curr Genomics.* 2009; 10:133–42. [PubMed: 19794886]
44. Nothwehr SF, Bruinsma P, Strawn LA. Distinct domains within Vps35p mediate the retrieval of two different cargo proteins from the yeast prevacuolar/endosomal compartment. *Mol Biol Cell.* 1999; 10:875–90. [PubMed: 10198044]
45. Hierro A, et al. Functional architecture of the retromer cargo-recognition complex. *Nature.* 2007; 449:1063–7. [PubMed: 17891154]
46. Seaman MN. Identification of a novel conserved sorting motif required for retromer-mediated endosome-to-TGN retrieval. *J Cell Sci.* 2007; 120:2378–89. [PubMed: 17606993]
47. Arighi CN, Hartnell LM, Aguilar RC, Haft CR, Bonifacino JS. Role of the mammalian retromer in sorting of the cation-independent mannose 6-phosphate receptor. *J Cell Biol.* 2004; 165:123–33. [PubMed: 15078903]
48. Eaton S. Retromer retrieves wntless. *Dev Cell.* 2008; 14:4–6. [PubMed: 18194646]
49. Verges M, et al. The mammalian retromer regulates transcytosis of the polymeric immunoglobulin receptor. *Nat Cell Biol.* 2004; 6:763–9. [PubMed: 15247922]

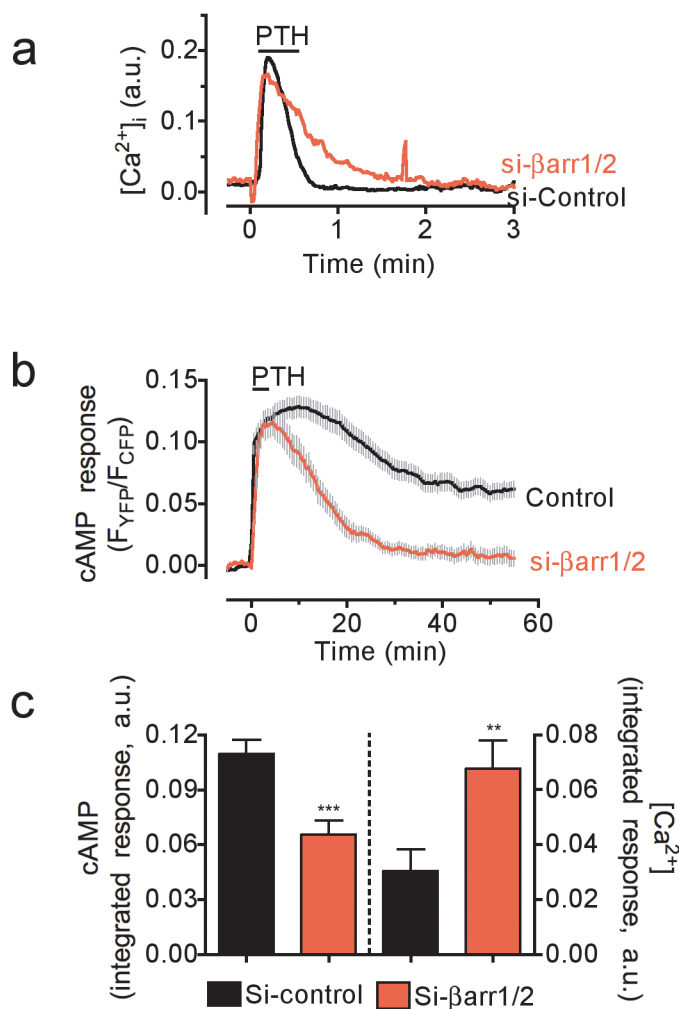


Figure 1. Time courses of cAMP and calcium responses to PTHR

a, HEK293 cells stably expressing PTHR were transfected with either si-RNA targeting both human β -arrestin1 and 2 (si- β Arr1/2) or scrambled siRNA. Changes in the intracellular levels of Ca^{2+} in response to 100 nM PTH(1–34) were measured by epifluorescence imaging at 488 nm excitation. Traces are representatives $N = 4$ independent experiments and $n = 28$ (control), and $n = 45$ (si- β arr1/2) cells.

b, Averaged cAMP response over a 50-min time course measured by FRET changes from HEK293 cells stably expressing PTHR and transiently expressing the cytoplasmic cAMP FRET sensor epac^{CFP/YFP}. Cells were continuously perfused with control buffer or 100 nM PTH1–34 (horizontal bar). Data represents the mean \pm s.e.m. of $N = 4$ independent experiments and $n = 25$ (control), and $n = 20$ (si- β arr1/2) cells.

c, Bars represent the average calcium and cAMP responses for experiments represented in (a) and (b), respectively, determined by measuring the area under the curve from 0–3 min for calcium response, and 0–30 min for cAMP. Statistical analysis was performed by a t-Test (***, $P < 0.001$; **, $P < 0.05$).

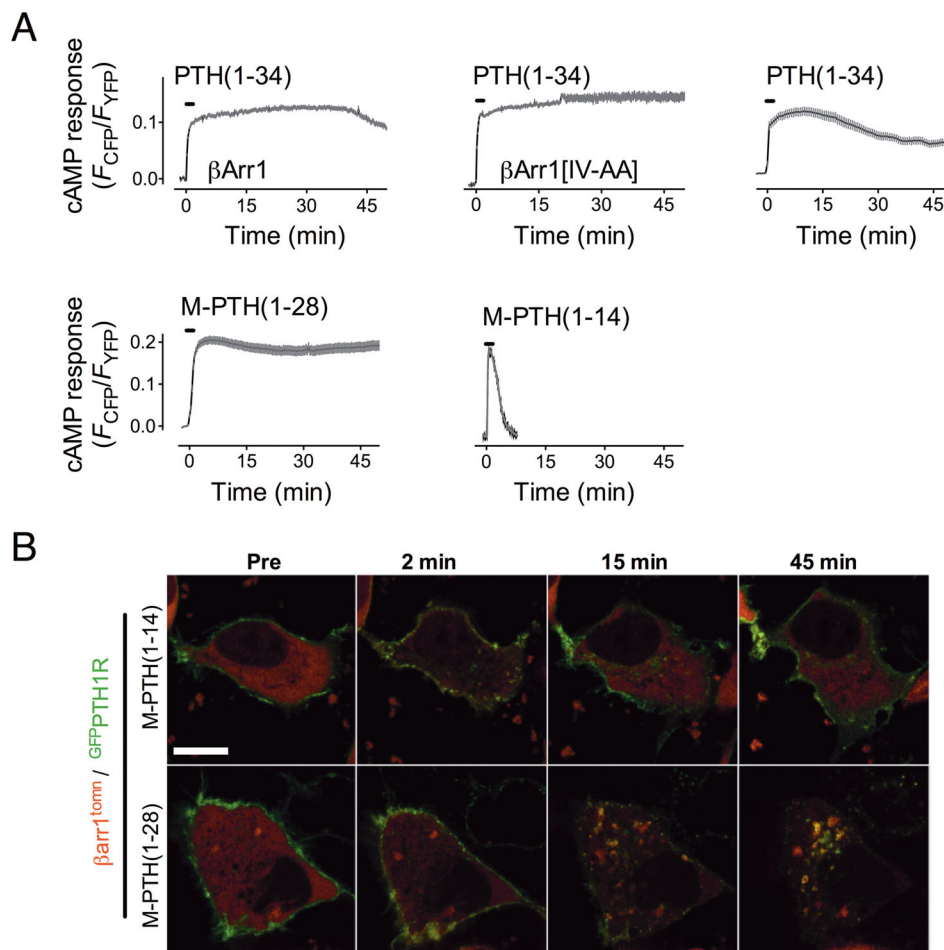


Figure 2. Signaling and arrestin mobilization by PTH analogs

a–b, Averaged cAMP response over a 45-min time course measured by FRET change from HEK293 cells stably expressing PTHR and transiently expressing Epac-CFP/YFP. Cells were continuously perfused with control buffer or 100 nM of ligand (horizontal bars) Data represents the mean \pm s.e.m. of $N = 5$ independent experiments and cell number $n = 25$ for PTH(1–34), $n = 10$ for M-PTH(1–14), $n = 44$ for M-PTH(1–28), $n = 18$ for β arr1, and $n = 13$ for β arr1[IV-AA].

c, PTHR-arrestin dynamics induced by PTH analogs. HEK293 cells were co-transfected with GFP^N-PTH1R and wild-type β -arr1^{tom} or β -arrestin 1[IV-AA]^{tom} and imaged at 1 min intervals for 1 h after a brief challenge with 100 nM PTH(1–34). The horizontal white bar represent 10 μ M.

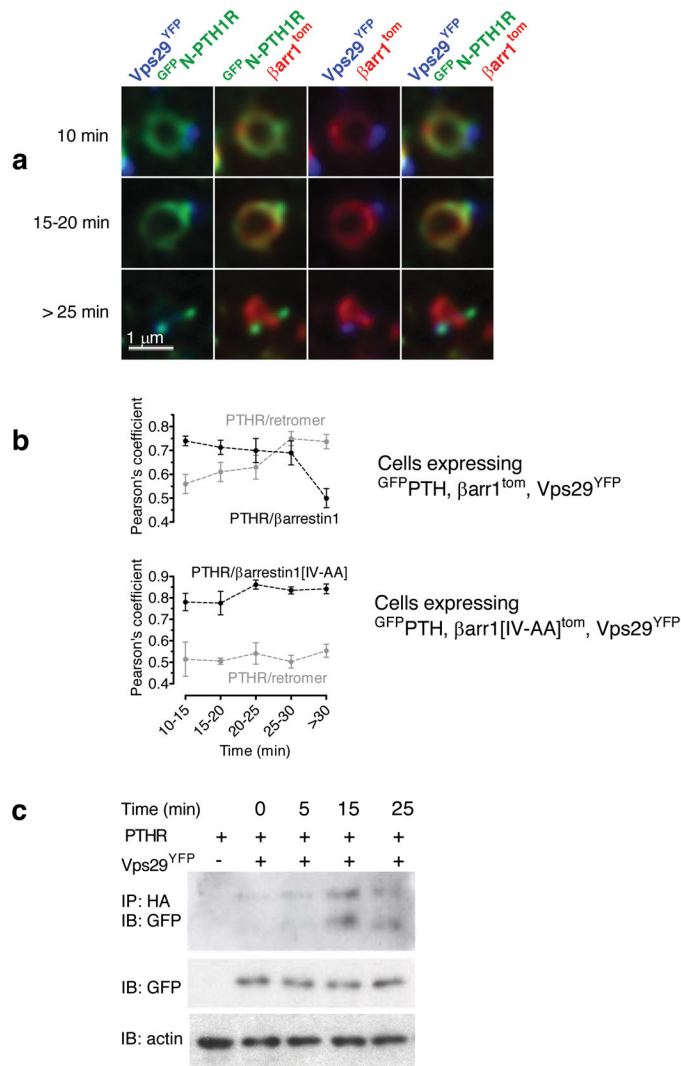


Figure 3. Retromer terminates the PTH-mediated cAMP response

a, Time-course of endosomal co-localization between PTHR, arrestin and retromer. HEK293 cells cotransfected to express GFPPTH, Vps29^{YFP} and β-arr1^{tom} were challenged with a brief pulse of PTH(1–34) (100 nM), and endosomes were visualized on a confocal microscope using spectral and spatial deconvolution. Representative endosomes showed characteristic colocalization patterns of GFPPTH, Vps29^{YFP} and β-arr1^{tom} at early (<15 min), medium (15–20 min) and late (>25 min) time points after ligand challenge. The horizontal white bar represent 1 μM.

b, Quantitative analysis of experiments in a. Individual endosomes were classified according to time after ligand challenge and colocalization (Pearson's, JACoP plugin, ImageJ) was measured for each endosome. Data represent the mean ± s.e.m of $N = 4$ independent experiments and $n = 19$ cells. We used a Pearson's analysis to quantify the change of PTHR localization from arrestin- to retromer-labeled endosomal domains. For each individual endosome, simultaneously labeled with GFPPTH/Vps29^{YFP}/β-arr1^{tom} or with GFPPTH/Vps29^{YFP}/β-arr1[IV-AA]^{tom}, we measured the Pearson's correlation coefficients for the colocalization between PTHR and arrestin, and between PTHR and retromer.

c, PTHR-retromer interaction detected using co-immunoprecipitation. HEK293 cells co-transfected with HA-PTHR and either empty vector or Myc-Vps26 and Vps29^{YFP} were challenged with carrier or with 100 nM PTH(1–34) for the designated time period at room temperature before lysis in ice-cold immunoprecipitation buffer. PTHR was immunoprecipitated with sepharose beads conjugated to anti-HA monoclonal antibody, and Vps29^{YFP} was detected with a polyclonal antibody against GFP ($n = 4$).

Author Manuscript

Author Manuscript

Author Manuscript

Author Manuscript

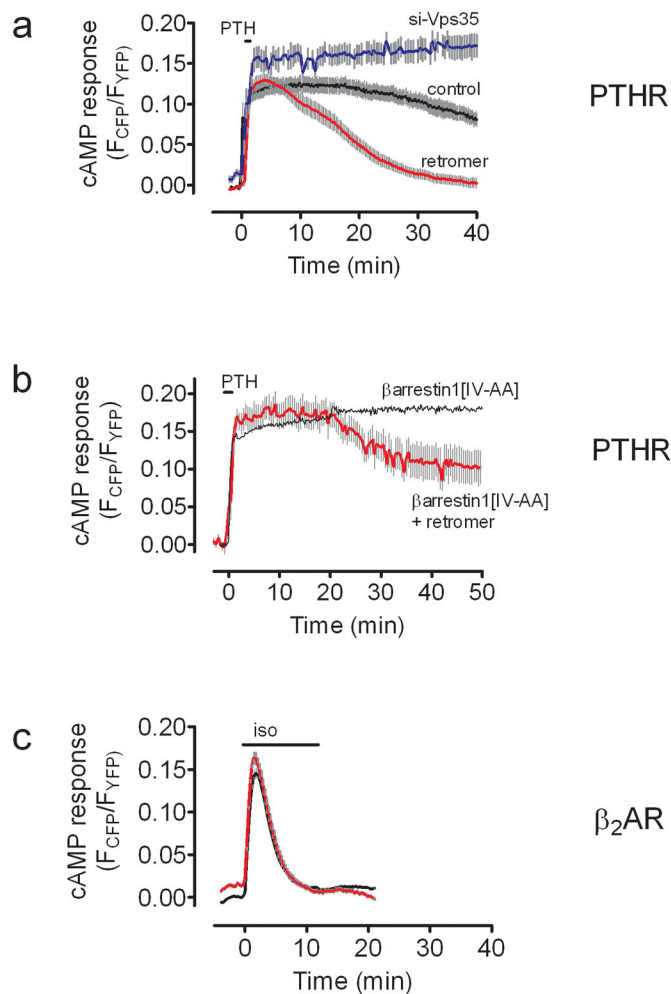


Figure 4. Modulation of PTHR signaling by retromer

a–b, Averaged cAMP response time-course measured by FRET changes from HEK-293 cells stably expressing PTHR (control, black), and transiently transfected to express (a) Vps26 and Vps29 (retromer, red), or siRNA of Vps35, and (b) β arr1[IV-AA]. Data represent the mean \pm s.e.m of $N = 4$ independent experiments and cell number $n = 10$ (control), $n = 15$ (retromer), $n = 15$ (si-Vps35), and $n = 9$ (retromer + β arr1[IV-AA]).

c, Averaged cAMP response time-course measured by FRET changes from HEK-293 cells expressing β_2 -AR alone (control, black), or in combination with Vps26 and Vps29 (retromer, red). Data represent the mean \pm s.e.m of $N = 4$ independent experiments and cell number $n = 20$ (control), and $n = 20$ (retromer). Cells were continuously perfused with control buffer or 100 nM PTH(1–34) (a,b), or 10 mM isoproterenol (c) (horizontal bar).

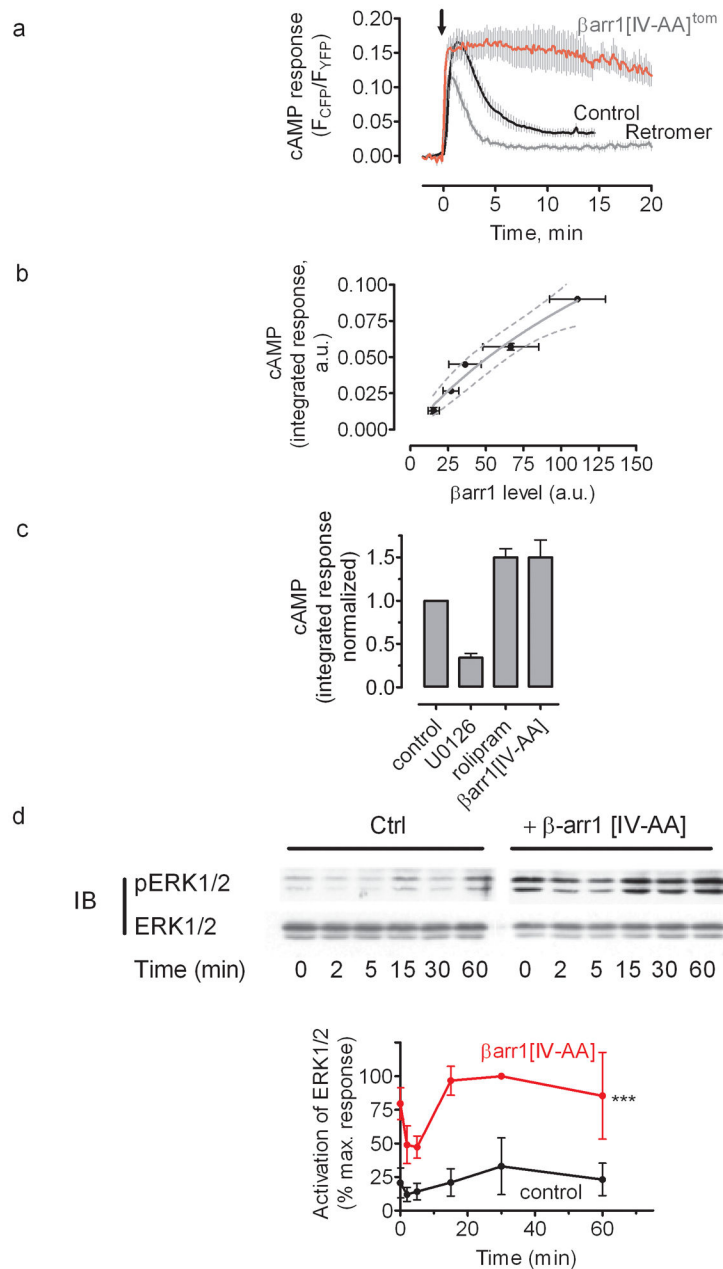


Figure 5. Retromer and arrestin regulate PTH-mediated cAMP production in bone cells
a, Averaged cAMP response measured by FRET changes in ROS17/2.8 cells expressing either epac^{CFP/YFP} alone or co-expressing epac^{CFP/YFP} with either β -arrestin1[IV-AA]^{tom} or Vps26 and Vps29. Cells were treated with control buffer or a brief challenge of 100 nM PTH(1–34) (arrow). Data represent the mean \pm s.e.m. of $N = 4$ independent experiments and $n = 20$ cells.

b, Expression level of wild-type β -arrestin1 influences cAMP signaling. ROS cells co-transfected with epac^{CFP/YFP} and β -arrestin1^{tom} were challenged with PTH (100 nM) as in (a) and time-courses of cAMP response were measured as described in Figure 1. Integrated signaling was estimated by summing the area under the curve from 0–15 min after ligand

challenge. Arrestin expression levels were estimated by epifluorescence imaging of tdTomato fluorescence. Integrated cAMP values were then binned according to arrestin expression level and plotted as averages (mean \pm s.e.m. $N = 4$ independent experiments). The dotted line represents the 95% confidence interval.

c, The total PTH-induced cAMP responses for experiments represented in the Supplementary Figure 6 were determined by measuring the area under the curve from 0–10 min. Bars represent the mean \pm s.e.m. of $N = 4$ independent experiments and $n = 12$ (control), $n = 14$ (U0126), $n = 15$ (rolipram), and $n = 20$ (β arr1[IV-AA]) cells.

d, Representative Western blots of time courses of ERK1/2 activation in ROS 17/2.8 cells control (Ctrl) or transiently transfected to express β arr1[IV-AA] in response to 100 nM PTH(1–34). The data are the mean \pm s.e.m. of $N = 3$ separate experiments; Statistical comparison of the curves was performed by a two-way ANOVA (***, $P < 0.001$).

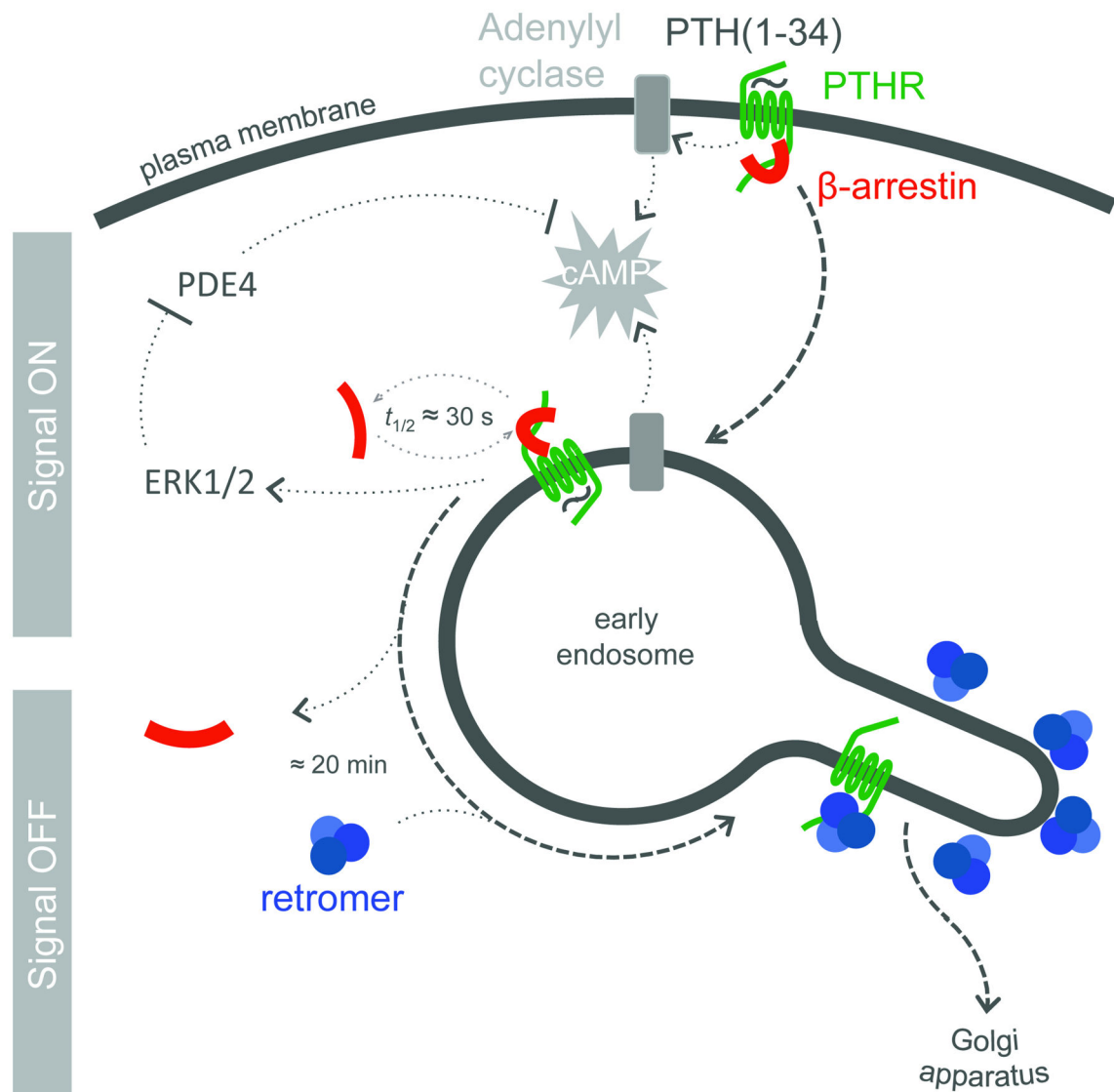


Figure 6.

Mode of regulation of PTHR signaling by retromer and arrestin. PTH-activated PTHR (green) generating cAMP (grey) by activation of adenylyl cyclases internalizes to endosomes in a process that involves binding of β -arrestin (red). Activated PTHR is then maintained in the early endosome bulk compartment by arrestin binding, where arrestin-mediated activation of ERK1/2 signaling causes inhibition of phosphodiesterases and permits sustained cAMP signaling. Binding of PTHR and retromer (blue) causes sorting of the receptor to retrograde trafficking domains. Generation of cAMP is stopped after either retromer binding in the retrograde domain or after retromer-mediated traffic to the Golgi.